The Company of
Biologists

RESEARCH ARTICLE

Erk and MAPK signaling is essential for intestinal development through Wnt pathway modulation

Gaigai Wei[1],[*], Na Gao[*],[1], Jiwei Chen[1], Lingling Fan[1], Zhiyang Zeng[1], Ganglong Gao[2], Liang Li[1], Guojiu Fang[2], Kewen Hu[1], Xiufeng Pang[1], Heng-Yu Fan[3], Hans Clevers[4], Mingyao Liu[1], Xueli Zhang[1,2,‡] and Dali Li[1,‡]

ABSTRACT

Homeostasis of intestinal stem cells (ISCs) is maintained by the orchestration of niche factors and intrinsic signaling networks. Here, we have found that deletion of Erk1 and Erk2 (Erk1/2) in intestinal epithelial cells at embryonic stages resulted in an unexpected increase in cell proliferation and migration, expansion of ISCs, and formation of polyp-like structures, leading to postnatal death. Deficiency of epithelial Erk1/2 results in defects in secretory cell differentiation as well as impaired mesenchymal cell proliferation and maturation. Deletion of Erk1/2 strongly activated Wnt signaling through both cell-autonomous and non-autonomous mechanisms. In epithelial cells, Erk1/2 depletion resulted in loss of feedback regulation, leading to Ras/Raf cascade activation that transactivated Akt activity to stimulate the mTor and Wnt/β-catenin pathways. Moreover, Erk1/2 deficiency reduced the levels of Indian hedgehog and the expression of downstream pathway components, including mesenchymal Bmp4 – a Wnt suppressor in intestines. Inhibition of mTor signaling by rapamycin partially rescued Erk1/2 depletion-induced intestinal defects and significantly prolonged the lifespan of mutant mice. These data demonstrate that Erk/Mapk signaling functions as a key modulator of Wnt signaling through coordination of epithelial-mesenchymal interactions during intestinal development.

KEY WORDS: Intestinal stem cell, Wnt signaling, Mesenchymal cell, Hedgehog signaling, MAPK

INTRODUCTION

Adult stem cells are crucial for cell proliferation and regeneration of differentiated cells during tissue homeostasis. The intestinal epithelium undergoes rapid cell turnover, and well-controlled cell differentiation and maturation, making it an excellent system for studying adult stem cell function and self-renewal. The maintenance of epithelial self-renewal is supported by two populations of intestinal stem cells (ISCs): Lgr5-positive fast-cycling crypt base columnar (CBC) stem cells wedged between Paneth cells (Barker et al., 2007); and quiescent +4 stem cells located just above the Paneth cells (Sangiorgi and Capecchi, 2008). Recently, increasing evidence suggests that +4 stem cells are very likely secretory progenitors (van Es et al., 2012) and should be considered a 'facultative stem cell' (Visvader and Clevers, 2016). More recently a novel damage-induced quiescent cell type called the revival stem cell has been identified; it is probably not a regular ISC because it is rarely found under homoeostatic conditions (Ayyaz et al., 2019). ISCs constantly generate transit-amplifying (TA) cells that further differentiate into postmitotic absorptive lineage (enterocytes) and secretory lineage (goblet cells, Paneth cells, enteroendocrine cells, Tuft cells, etc.) cells in the small intestine. Stem cell hierarchies in the small intestine are rigorously controlled by the orchestration of reciprocal niche signals from neighboring Paneth cells and underlying mesenchymal cells (Sato et al., 2011; Clevers, 2013).

The maintenance of ISCs and tissue homeostasis is tightly orchestrated by several crucial signaling pathways. Wnt signaling is the essential driving force supporting ISCs and maintaining the crypts as well as inducing Paneth cell maturation (van Es et al., 2005a; Liu et al., 2013). In cooperation with Wnt signaling, the Notch (Fre et al., 2009; van Es et al., 2005b) and EGF (Wong et al., 2012; Miettinen et al., 1995) pathways promote crypt expansion and regulate cell differentiation. In contrast, the BMP (He et al., 2004; Haramis et al., 2004) and hedgehog (Kosinski et al., 2010; Akiyoshi et al., 2006) pathways negatively regulate epithelial Wnt signaling to promote cell differentiation. Moreover, epithelial cells secrete hedgehog, mainly Indian hedgehog (Ihh), to induce mesenchymal BMP production, which is crucial for epithelial-mesenchymal interactions and crypt formation (Ramalho-Santos et al., 2000). However, it is still obscure how the Ihh pathway is regulated by upstream signals in the intestinal epithelium.

The mitogen-activated protein kinase (MAPK) pathway, a downstream signaling target of EGF and other mitogens, plays pivotal roles in regulating intestinal epithelial cell (IEC) growth, Paneth versus goblet cell choice and the ISC population; however, the underlying mechanism is still disputed (Haigis et al., 2008; Trobridge et al., 2009; Heuberger et al., 2014; de Jong et al., 2016). Intestinal-specific deletion of the MAPK pathway upstream activator Shp2 promotes Paneth cell differentiation and expands the ISC pool through activation of the Wnt pathway (Heuberger et al., 2014). Expression of the constitutively active G12 V mutant Kras in mouse intestines promotes goblet cell differentiation in a Notch pathway-dependent manner, but does not affect stem cells and the Wnt signaling pathway (Feng et al., 2011). It suggests that the role of MAPK signaling in intestinal homeostasis is complicated and individual components of this cascade may have distinct physiological functions in intestinal homeostasis.

As one of the major direct targets of the Ras-Raf-MEK cascade, the extracellular signal-regulated kinases 1 and 2 (Erk1/2) are crucially involved in multiple physiological and pathological functions in various tissues, including embryonic development, reproduction, T cell development, immunoregulation and tumorigenesis (Yao et al., 2003; Fan et al., 2009; Fischer et al., 2005). *Erk1* and *Erk2* are

[1]Shanghai Key Laboratory of Regulatory Biology, Joint Research Center for Translational Medicine, ECNU-Fengxian Hospital, Institute of Biomedical Sciences and School of Life Sciences, East China Normal University, Shanghai 200241, China. [2]Fengxian Hospital affiliated to Southern Medical University, Shanghai 201499, China. [3]Life Sciences Institute, Zhejiang University, Hangzhou 310058, China. [4]Hubrecht Institute, Royal Netherlands Academy of Arts and Sciences (KNAW), Uppsalalaan 8, Utrecht 3584 CT, The Netherlands.
*These authors contributed equally to this work

‡Authors for correspondence (dlli@bio.ecnu.edu.cn; lejing1996@aliyun.com)

X.Z., 0000-0002-7741-1081; D.L., 0000-0002-0679-8477

DEVELOPMENT

homologous genes with distinct functions during embryonic development, but in the majority of the tissues they mainly play redundant roles. Recently, it was reported that IEC-specific depletion of Erk1/2 in adult mice results in dysregulated epithelial cell migration, secretory cell differentiation and nutrient absorption with aberrant Erk5 activation (de Jong et al., 2016). Although Erk5 activation could partially explain the Erk1/2 depletion-induced cell proliferation and migration phenotype, it is still not clear how Erk1/2 regulates the cell differentiation and morphology changes that are crucial for intestinal homeostasis. To further understand the physiological function of Erk1/2 at earlier stages, we deleted Erk1/2 in IECs during embryonic stages using Villin-Cre, and found dramatic expansion of the ISC population, impaired secretory lineage differentiation and enterocyte maturation leading to postnatal lethality. Unexpectedly, Erk1/2 deficiency also stimulated hyperproliferation and migration of epithelial cells, and caused profound morphological changes to polyp-like structures in the small intestines in postnatal mice. Most of the defects in Erk1/2 mutant intestines were attributed to strongly activated Wnt signaling through decreased Ihh production and Ras/Akt/mTOR signaling activation, due to loss of Erk1/2-mediated feedback inhibition. Our study demonstrates that Erk1/2 plays a crucial role during intestinal development through modulation of the Wnt signaling pathway through both cell-autonomous and non-autonomous mechanisms.

RESULTS

Deficiency of Erk1/2 in IECs disrupts epithelial morphology and leads to postnatal lethality

Previous studies have shown that active Erk1/2 is localized in the TA zone of the crypt (de Jong et al., 2016). Through immunofluorescence staining, we found that, in addition to TA cells, phospho-Erk (p-Erk)-positive cells also colocalized with Lgr5-positive ISCs, which expressed eGFP in intestinal tissue of adult *Lgr5-eGFP-IRES-creERT2* mice (Barker et al., 2007) (Fig. 1A). In the embryonic stages, Erk is activated uniformly throughout the IECs (Fig. 1B) as ISCs and progenitors occupy the entire intestinal epithelium during embryonic development. These data suggest that Erk/MAPK signaling is activated in highly proliferating IECs during development and adulthood. To analyze the function of Erk1/2 signaling in intestinal development, compound genetically modified mice were generated by crossing $Erk1^{-/-};Erk2^{fl/fl}$ (Fischer et al., 2005; Pages et al., 1999), as we previously described (Fan et al., 2009), with Villin-Cre transgenic mice (Madison et al., 2002) (referred to as $Erk^{\Delta IEC}$ hereafter). Tissue-specific depletion of Erk1/2 was confirmed by immunofluorescence and immunohistochemistry (Fig. S1A).

The body size of newborn $Erk^{\Delta IEC}$ mice was similar to littermate controls (data not shown) but the subsequent weight gain was dramatically reduced in $Erk^{\Delta IEC}$ pups, probably owing to poor nutrition status because Erk1/2 was specifically deleted in intestinal epithelial cells (Fig. 1C). Although the time of lethality varied, all of the $Erk^{\Delta IEC}$ pups died within 30 days, demonstrating an essential role for Erk signaling in IECs, as previously reported for deletion of Erk1/Erk2 in adult mice (de Jong et al., 2016). Through histological analysis of tissues from P14 mice, we found that the morphology of the entire intestine was severely disrupted in $Erk^{\Delta IEC}$ mice (Fig. S1B). In some particular sites, branched villi were observed in the small intestine of $Erk^{\Delta IEC}$ mice (Fig. 1D), and the morphology of the colon was also disorganized with polyp-like structures (Fig. 1E). As determined by scanning electron microscope (SEM), irregular
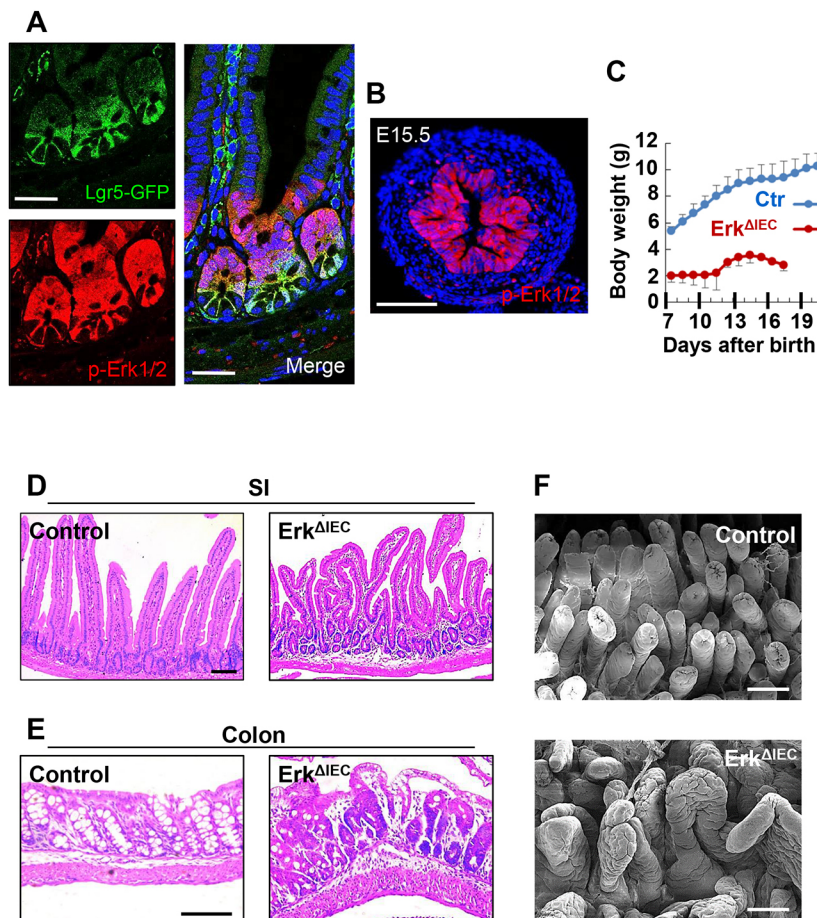
Fig. 1. Loss of Erk1/2 disrupted intestinal epithelial morphology. (A) Immunofluorescence analysis of Lgr5-eGFP (green) and p-Erk1/2 (red) in the adult small intestine of *Lgr5^{eGFP-IRES-creERT2}* mice. (B) Immunofluorescence staining for p-Erk1/2 in intestines of wild-type mice at embryonic day 15.5. (C) Loss of Erk1/2 significantly reduced mouse body weight. Graph shows the average body weight of control and $Erk^{\Delta IEC}$ mice from P7 to P18. Data are mean±s.e.m. (*n*=5). (D,E) Deletion of Erk1/2 resulted in disruption of intestinal morphology. Hematoxylin and Eosin staining of both proximal small intestine (SI) and colon from control and $Erk^{\Delta IEC}$ littermates at P14. (F) Scanning electron microscopy for proximal small intestine of control and $Erk^{\Delta IEC}$ littermates at P14. Scale bars: 25 μm in A; 100 μm in B,D-F.

projections of fused giant villi were formed in $Erk^{\Delta IEC}$ small intestines but not in controls (Fig. 1F). Further analysis showed that no obvious morphological defects were observed until P7, and deletion of Erk1 in mice did not affect intestinal development (Fig. S1C,D). These data suggest that Erk signaling plays a pivotal role in regulation of intestine morphology during development.

Abrogation of Erk1/2 stimulates cell proliferation and migration

Numerous studies have shown that the Erk/MAPK pathway is crucial for cell proliferation; therefore, we assumed that ablation of Erk would inhibit intestinal cell growth. To our surprise, the number of Ki67$^+$ proliferating cells was dramatically increased in both the small intestine and colon of $Erk^{\Delta IEC}$ mice, and the crypts were swollen with increased size in $Erk^{\Delta IEC}$ mice compared with controls (Fig. 2A). Increased cell proliferation in $Erk^{\Delta IEC}$ intestines was first observed at postnatal day 7, but not in embryonic stages and P0 (Fig. S2A). Progenitors in the crypts proliferate quickly and migrate toward the villi. To determine whether the expanded number of proliferating cells in crypts is due to a reduction in cell migration rate, BrdU pulse-chase experiments were performed. We found that the cells in $Erk^{\Delta IEC}$ mice exhibited a much faster migration rate from the crypt to villus in both small intestine and colon tissues (Fig. 2B; Fig. S2B). To determine whether this phenotype is a cell-autonomous function of Erk signaling in epithelial cells, the small intestinal organoid culture system was employed (Sato et al., 2009). Isolated $Erk^{\Delta IEC}$ organoids were much larger than controls, consistent with the above observation of expanded crypts in $Erk1/2^{\Delta IEC}$ mice (Fig. 2C). Through consecutive monitoring of single live organoids, the growth rate and the number of budding protrusions were dramatically increased in $Erk^{\Delta IEC}$ organoids (Fig. 2C), which was further confirmed by EdU labeling (Fig. 2D). These data demonstrate that Erk1/2 has a cell-autonomous role in limiting IEC cell proliferation and migration.

Erk signaling controls secretory lineage differentiation and stem cell population

Next, we analyzed the role of Erk1/2 in intestinal epithelial cell differentiation. Consistent with previously reports (de Jong et al., 2016), ablation of Erk1/2 in IECs led to impaired secretory lineage differentiation and maturation. A dramatically increased number of Paneth cells with disordered localization was observed in P14 $Erk^{\Delta IEC}$ intestines (Fig. 3A). Moreover, premature Paneth cells were present in P6 $Erk1/2^{\Delta IEC}$ mice but not in the controls (Fig. S3A). In $Erk^{\Delta IEC}$ intestines, the number of goblet cells, but not enteroendocrine cells, was significant decreased (Fig. 3B; Fig. S3B,C). The number of Tuft cells, a rare secretory lineage cell type initiating anti-parasite type 2 immunity in the intestines (Gerbe et al., 2016), was dramatically reduced, as determined by immunostaining for the specific maker Dclk1 and the mRNA expression levels of other Tuft cell markers, such as Chat, Trpm5 and Ptgs1 (Haber et al., 2017) (Fig. S3D-F). The number of alkaline phosphatase (AP)-positive enterocytes was reduced and AP activity declined in $Erk^{\Delta IEC}$ mice compared with controls. It demonstrates that the differentiation and maturation of absorptive enterocytes of the $Erk^{\Delta IEC}$ mice is inhibited (Fig. S3G). Moreover, through SEM analysis, the enterocyte brush border microvilli were sparse, short and thin in $Erk^{\Delta IEC}$ mice (Fig. S3H), suggesting an impaired absorption function, which is probably a major reason why mutant mice were lean and malnourished.

As active Erk1/2 was observed in ISCs (Fig. 1A), we investigated whether ISCs were affected in $Erk1/2^{\Delta IEC}$ intestines. Olfm4-positive cells were clearly expanded in the crypts of $Erk^{\Delta IEC}$ intestines compared with controls both at P7 and P14 (Fig. 3C and Fig. S3I). Similar results
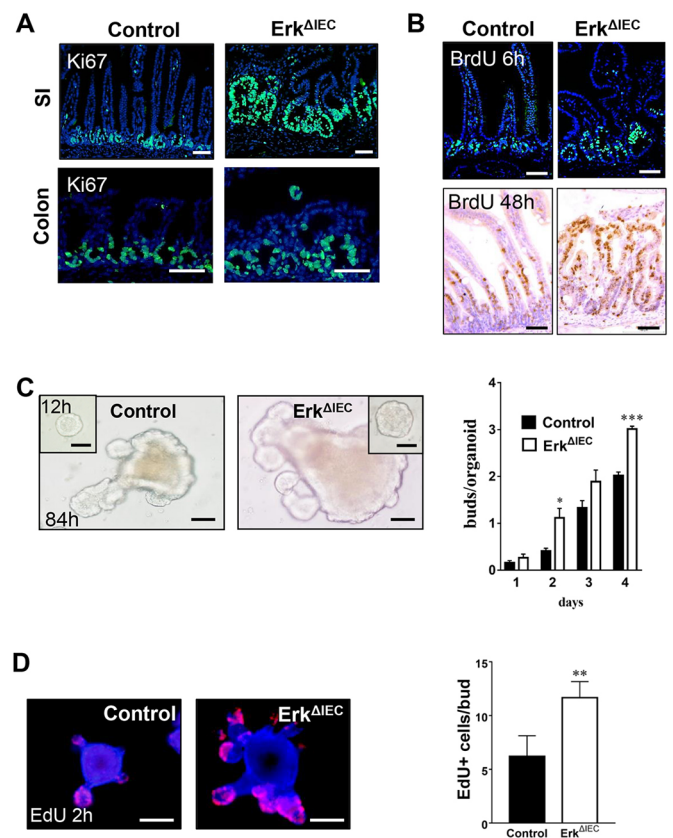

Fig. 2. Ablation of Erk1/2 in the intestine increased cell proliferation and migration. (A) Intestinal cell proliferation was increased in Erk$^{\Delta IEC}$ mice compared with control littermates. Immunofluorescence staining with antibody against Ki67 (green) in intestines of control and Erk$^{\Delta IEC}$ littermates at P14. (B) Loss of Erk1/2 stimulated intestinal epithelial cell migration. BrdU was injected into 2-week-old control and Erk$^{\Delta IEC}$ littermates. BrdU incorporated into intestinal cells (green) was visualized via immunofluorescence staining 6 h (top) and immunohistochemical staining 48 h (bottom) after injection. (C) Erk1/2-deficient intestinal organoids grew faster than controls. Organoids derived from 2-week-old mice of each genotype were cultured and the growth of single organoids was photographed at consecutive time points. Representative images of organoids cultured for 12 h (insets) and 84 h are presented. Quantification of average number of buds per organoid. Data are mean±s.e.m. (n=3 mice per group and a total of 90 organoids were analyzed for each genotype). *P<0.05, ***P<0.001; t-test. (D) Deletion of Erk1/2 stimulated cell proliferation in organoid culture. Organoids derived from 2-week-old control and Erk$^{\Delta IEC}$ littermates were labeled with EdU for 2 h and the images were taken using a fluorescent microscope. Quantification of Edu$^+$ cells per bud (n=3 mice per group and a total of 90 organoids were analyzed for each genotype). Scale bars: 50 μm.

were also observed in Erk1/2 mutant *Lgr5-eGFP-IRES-creERT2* mice, as determined by staining of Lgr5-GFP positive cells (data not shown). Expansion of ISCs was further supported by real-time qRT-PCRs, which showed that levels of common ISC markers such as Ascl2 (van der Flier et al., 2009), Aqp1 and Smoc2 (Munoz et al., 2012), were significantly increased (Fig. 3D and Fig. S3J). These data suggest that Erk signaling is crucial for intestinal epithelial cell differentiation, including the choice between enterocyte and secretory cell lineages, as well as for controlling terminal differentiation in the secretory lineage. Moreover, Erk is also important for maintaining the ISC population.

Epithelial Erk signaling regulates the intestinal mesenchymal compartment

As shown in Fig. 1, deletion of Erk1/2 in epithelial cells leads to disruption of the villus structure, which is controlled by the interaction
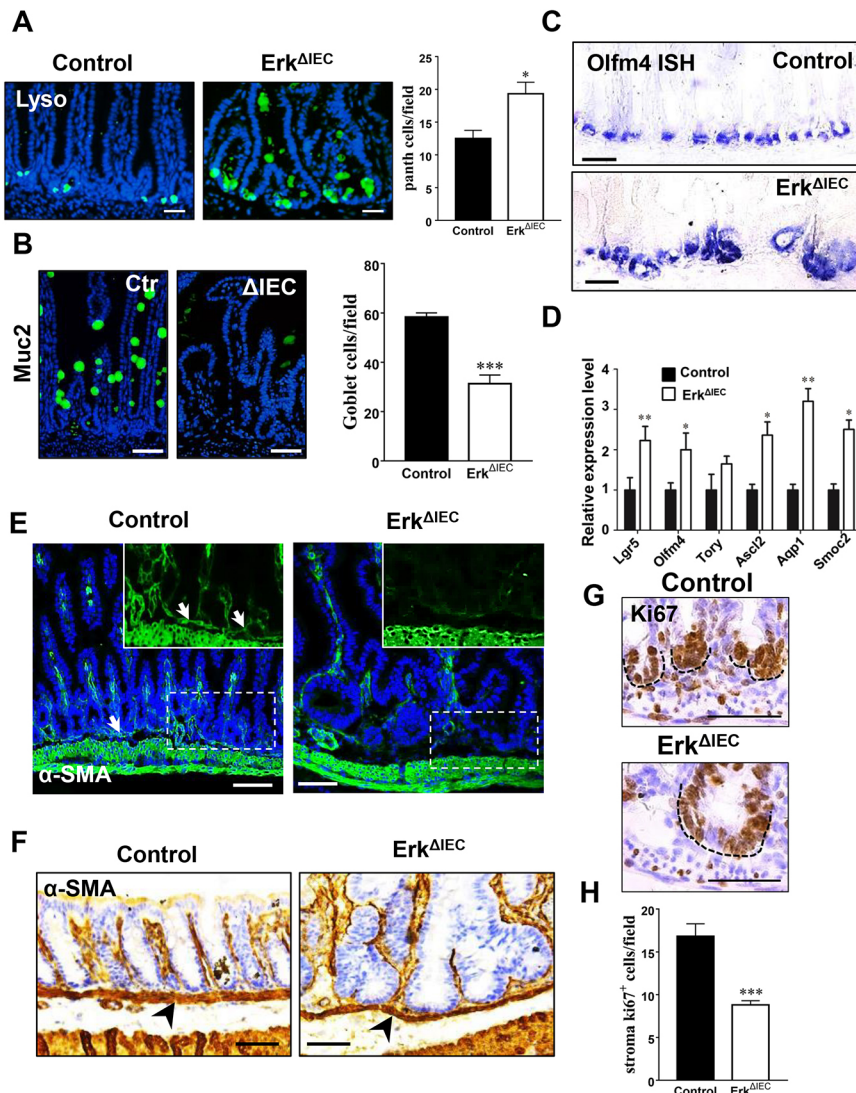
Fig. 3. Erk1/2 regulates IEC differentiation, stem cell population and mesenchymal cell maturation.
(A) Paneth cells were detected by staining with an antibody against lysozyme (green); numbers were increased in Erk$^{\Delta IEC}$ mice compared with control littermates. Quantification of Paneth cells (n=4 mice per group and lyso$^+$ cells were counted in 20 fields for each genotype). Data are mean±s.e.m. *P<0.05; t-test. (B) The number of mucin 2 (Muc2)-positive goblet cells (green) was dramatically decreased in Erk$^{\Delta IEC}$ mice. Quantification of goblet cells (n=3 mice per group and Muc2$^+$ cells were counted in 20 fields for each genotype). Data are mean±s.e.m. ***P<0.001; t-test. (C) RNA *in situ* hybridization analysis of Olfm4 mRNA in control and Erk$^{\Delta IEC}$ littermates. (D) ISC marker gene mRNA levels in wild-type and Erk$^{\Delta IEC}$ small intestines from P6 mice were determined by qRT-PCR. Data are mean±s.e.m. *P<0.05, **P<0.01; t-test. (E,F) Disrupted muscularis mucosae cells in Erk$^{\Delta IEC}$ intestinal tissues. α-Smooth muscle actin (α-SMA) immunostaining analysis of control and Erk$^{\Delta IEC}$ small intestine (G) and colon (H) tissues at P14. Arrowheads indicate intestinal muscularis mucosa. Muscularis mucosa layer is thinner in Erk$^{\Delta IEC}$ colons compared with those of controls. (G) Decreased cell proliferation of mesenchymal cells in Erk$^{\Delta IEC}$ mice. Ki67 immunohistochemistry was performed in control and Erk$^{\Delta IEC}$ mice at P6. Black-dashed lines indicate crypt structures. (H) Quantification of proliferation cells in the mesenchymal zone (n=3 mice per group and Ki67$^+$ cells were counted in 20 fields for each genotype). ***P<0.001; t-test. Scale bars: 50 μm.

of both the epithelium and the mesenchyme underneath. We investigated the α-smooth muscle actin (α-SMA)-positive muscularis mucosa (MM) and found that the layer of α-SMA-positive MM beneath the crypts was absent in some parts of *Erk1/2*$^{\Delta IEC}$ small intestine but not in control mice (Fig. 3E). Further analysis showed that α-SMA-positive MM was smaller at postnatal day 7, but not at embryonic stages and P0 (Fig. S4A). Although α-SMA-positive MM constitutes a consecutive layer in colon tissues, the thickness of the layer was reduced in Erk mutant tissue (Fig. 3F). Mesenchymal cells in the villus core and pericryptal region underwent rapid proliferation postnatally. Both the number and the size of proliferating pericryptal cells were greatly reduced in *Erk*$^{\Delta IEC}$ mice compared with the controls at P6 (Fig. 3G,H). These data suggest that epithelial Erk signaling is crucial for intestinal subepithelial cell proliferation and maturation.

Activation of Wnt/β-catenin signaling in Erk$^{\Delta IEC}$ intestines

The perturbation of intestinal cell differentiation and ISC expansion observed in Erk$^{\Delta IEC}$ mice share a similar phenotype with intestinal-specific deletion of the *Apc* gene, which results in hyperactivation of Wnt/β-catenin signaling (Sansom et al., 2004). As shown in Fig. 4A, we found that the spectrum of cells expressing direct Wnt/β-catenin target genes, such as *Myc* and *Sox9*, was broader in Erk$^{\Delta IEC}$ intestines than in control intestines. Moreover, the expression level of another

Wnt target, cyclin D1, was dramatically elevated in Erk$^{\Delta IEC}$ intestinal tissues compared with controls (Fig. 4B). Consistently, more cells with a nuclear localized active form of β-catenin in Erk$^{\Delta IEC}$ crypts were observed (Fig. 4C). RNA-sequencing was performed to uncover the transcriptome profile of Erk$^{\Delta IEC}$ intestines versus controls. After analysis of the geneset of canonical Wnt target genes in the intestine (Van der Flier et al., 2007), we found that most of the Wnt/β-catenin-dependent genes were significantly upregulated in Erk$^{\Delta IEC}$ mice compared with controls (Fig. 4D), suggesting a global activation of Wnt downstream signaling.

It is well accepted that Wnt signaling activates the Notch pathway through transcriptional activation of Notch ligands, such as Dll1 and jagged 1, in development and colorectal cancer (Galceran et al., 2004; Rodilla et al., 2009). We found that the expression of both Notch ligands and downstream genes was dramatically elevated in Erk$^{\Delta IEC}$ intestines compared with controls (Fig. 4E). This suggests that the loss of goblet cells in Erk$^{\Delta IEC}$ is likely due to Wnt-induced Notch activation. To further confirm that Notch hyperactivation in Erk$^{\Delta IEC}$ intestines is due to elevated ligand expression, we used DBZ, a γ-secretase inhibitor, which attenuates Notch activation at the receptor level, to treat the mice. As a positive control, DBZ treatment increased the goblet cell number in the intestines of control mice. DBZ also restored the differentiation of goblet cells in
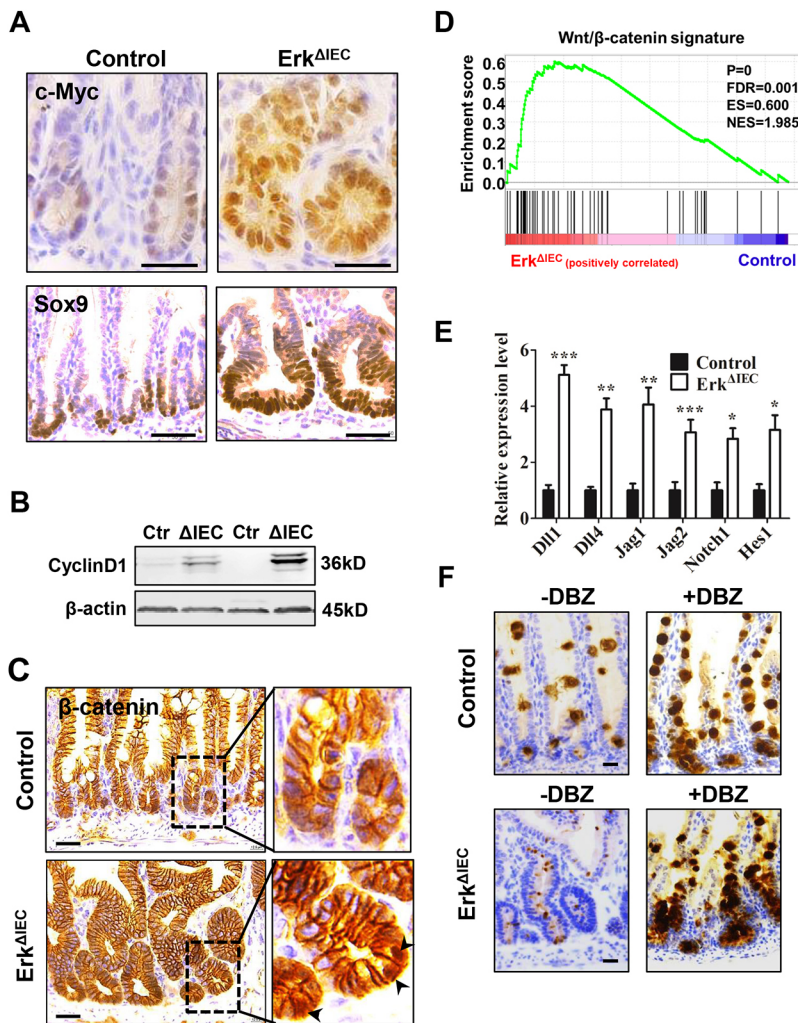
Fig. 4. Dramatic activation of Wnt signaling in Erk$^{\Delta IEC}$ **intestines.** (A) Immunohistochemical analysis for Myc (upper) and Sox9 (lower) in control and mutant littermates at P14. (B) The levels of cyclin D1 were determined by western blotting in intestinal samples harvested from control and Erk$^{\Delta IEC}$ mice at P14. β-Actin was used as a loading control. (C) β-Catenin staining in intestines from control and Erk$^{\Delta IEC}$ mice at P14. Arrowheads indicate nuclear β-catenin staining. (D) Gene set enrichment analysis (GSEA): plot of enrichment score of control versus Erk$^{\Delta IEC}$ intestinal tissue at P14 for the Wnt/β-catenin gene signature ($n=3$). (E) Quantitative real-time PCR analysis of Notch signaling component mRNA levels in small intestines of control and Erk$^{\Delta IEC}$ mice at P14. Data are mean±s.e.m. ($n=5$, *$P<0.05$, **$P<0.01$, ***$P<0.001$; t-test). (F) Inhibition of the Notch pathway rescued goblet cell differentiation in Erk$^{\Delta IEC}$ mice. Immunohistochemical analysis of Muc2 was performed in control and Erk$^{\Delta IEC}$ mice treated with or without the γ-secretase inhibitor DBZ for 10 days. Scale bars: 50 μm.

Erk$^{\Delta IEC}$ mice to a level similar to DBZ-treated controls (Fig. 4F). These data suggest that Erk deficiency induces Wnt signaling activation, which increases Notch ligand expression and Notch pathway activation to regulate secretory cell lineage differentiation.

Erk signaling deficiency induced the Akt-mTor pathway in epithelial cells

The phenotype of polyp-like morphology observed in Erk$^{\Delta IEC}$ intestines is similar to that in hamartomatous polyposis syndromes, which are usually caused by genetic mutations leading to activation of Akt/mTor signaling pathway in the gastrointestinal tract (Zbuk and Eng, 2007). To test whether Erk depletion induced Akt/mTor signaling, we examined the activity of this pathway in the intestines. The activity of Akt is not very strong in wild-type intestines, as previously described (He et al., 2007). In contrast, Erk$^{\Delta IEC}$ crypts contained many more crypt cells with stronger p-Akt staining signals than controls (Fig. 5A). As expected, elevated Akt activity also induced hyperactivation of mTor signaling, as shown by the p-S6 and p-4E-BP1 level in intestinal tissue. mTor activity is normally restricted to the crypt and lower part of the villus, but in Erk$^{\Delta IEC}$ mice, cells residing in the upper part of the villi exhibited stronger p-S6 and p-4E-BP1 staining as early as P7 (Fig. 5B,C and Fig. S5A). Further studies using western blotting also confirmed that the Akt/mTor pathway was strongly activated in Erk$^{\Delta IEC}$ intestines (Fig. 5D). It has been reported that Akt activates β-catenin through direct phosphorylation of Ser552, which promotes crypt expansion in intestines (He et al., 2007).

Activated Akt in Erk-deficient intestines also elevated the level of p-β-catenin Ser552 (Fig. 5D), suggesting that aberrant Akt activation is one of the factors driving Wnt hyperactivation in the Erk$^{\Delta IEC}$ intestine. To understand the reason why Erk deficiency induces Akt/mTor activation, we examined the activity of MAPK components upstream of Erk1/2, because many studies have demonstrated negative-feedback regulation of the MAPK pathway by Erk in cancer cells (Lake et al., 2016). Inhibition of Erk or Mek can activate the PI3K/Akt pathway via distinct mechanisms in many types of cancer (Lake et al., 2016; Zmajkovicova et al., 2013; Prahallad et al., 2012). We found that active Ras, Raf and Mek1/2 levels, but not Egfr levels, were dramatically elevated in Erk$^{\Delta IEC}$ intestines (Fig. 5E). This suggests that deletion of Erk1/2 results in activation of MAPK, probably downstream of the receptor. Immunohistochemistry studies also confirmed that Mek1/2 was activated in Erk$^{\Delta IEC}$ intestines, especially in tissue with malformed villi and crypts (Fig. 5F). However, ERK$^{\Delta IEC}$ organoids still required EGF in culture medium (data not shown), suggesting not fully functional activation of MAPK upon ERK depletion. These data suggest that hyperactivation of MAPK components, such as Ras and Raf, transactivates Akt signaling, as previously reported (Blalock et al., 2003; Lake et al., 2016).

Erk1/2 modulates BMP pathway through regulation of Ihh signaling

Deletion of Erk1/2 specifically in epithelial cells also impaired mesenchymal cell proliferation and maturation (Fig. 3), suggesting
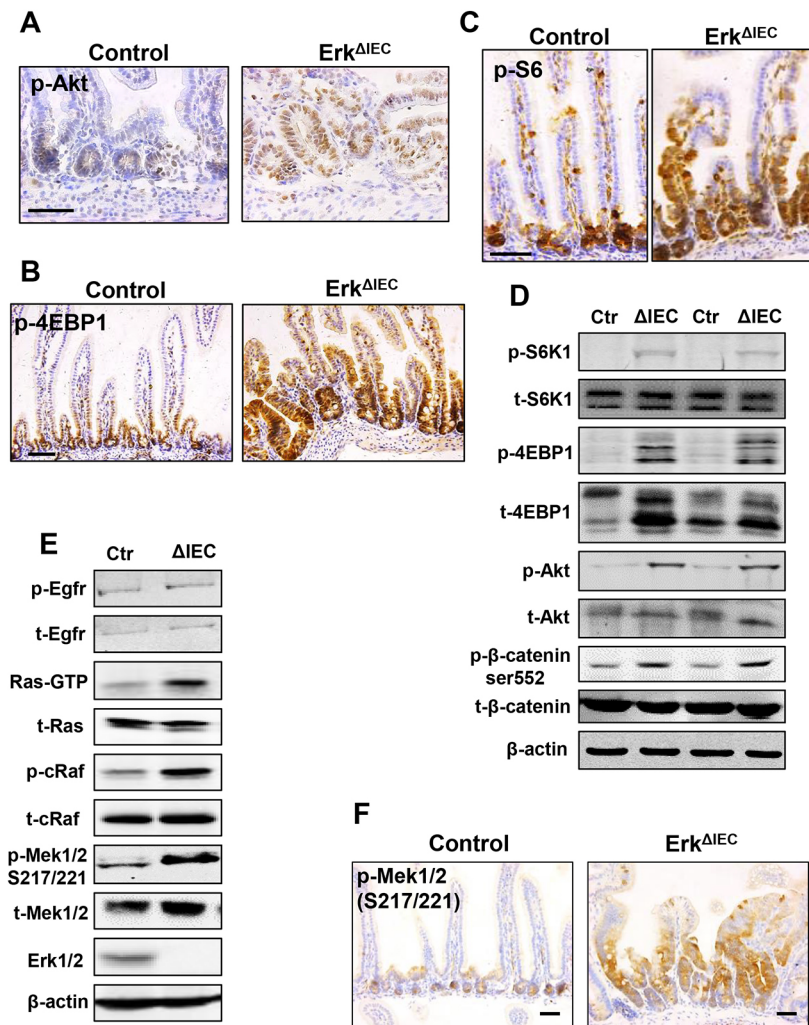
Fig. 5. Depletion of Erk1/2 in epithelial cells enhanced the Akt-mTOR pathway via activation of MAPK cascades. (A) Activation of Akt signaling in Erk$^{\Delta IEC}$ intestine. Immunohistochemical analysis of p-Akt in control and Erk$^{\Delta IEC}$ intestines at P14. (B,C) Loss of Erk1/2 enhanced the mTORC1 pathway in intestines. Immunohistochemical analysis of p-S6 (B) and p-4EBP1 (C) in control and Erk$^{\Delta IEC}$ intestines at P14. (D) Loss of Erk1/2 caused increased Akt-mTORC1 pathway component phosphoprotein levels. The level of p-Akt, p-S6K1, p-4EBP1 and p-β-catenin (S552) was determined by western blotting in intestinal samples harvested from control and Erk$^{\Delta IEC}$ mice at P14. β-Actin was used as loading control. (E) Activation of the Ras-Raf-Mek1 cascade in Erk1/2-depleted intestines. The levels of p-Egfr, Ras-GTP, p-Akt, p-Raf and p-Mek1 were determined by western blotting in intestinal samples harvested from control and Erk$^{\Delta IEC}$ mice at P14. β-Actin was used as loading control. (F) Immunohistochemical analysis for p-Mek1/2-S217/221 in control and Erk$^{\Delta IEC}$ intestines at P14. Scale bars: 50 μm in A,B,C,F.

that Erk regulates factors secreted by epithelial cells that function in the mesenchyme. We focused on hedgehog, as it is secreted from IECs and plays essential roles in intestinal development and villus patterning via its receptors in mesenchymal cells (Kosinski et al., 2010; Madison et al., 2005). Through analysis of the RNA-Seq data, we found that hedgehog signaling was dramatically impaired (Fig. 6A). A qRT-PCR assay demonstrated that mRNA levels of Ihh, as well as hedgehog pathway downstream targets, such as Hhip, Ptch1 and Gli1, were significantly reduced in Erk$^{\Delta IEC}$ intestines (Fig. 6B).

Immunohistochemistry studies revealed that the expression of Ihh was reduced in Erk$^{\Delta IEC}$ epithelial cells compared with controls (Fig. 6C). To confirm that Ihh expression is controlled by the Erk pathway in epithelial cells, organoids from both control and Erk$^{\Delta IEC}$ mice were cultured. Downregulation of Ihh expression was confirmed in mutant organoids using western blotting (Fig. 6D). Ptch1, the receptor and direct downstream target of the hedgehog pathway, was downregulated in Erk$^{\Delta IEC}$ mesenchymal cells (Fig. 6E). In the intestines, Bmp4 and its signaling are the major downstream effectors of the Ihh pathway responsible for intestinal morphology and function (Roberts et al., 1995; van Dop et al., 2009). We found that downregulation of Bmp4 protein was correlated with the Ihh level in Erk$^{\Delta IEC}$ intestinal tissues (Fig. 6F). Immunohistochemistry analysis demonstrated that phospho-Smad1/5/8 protein levels were greatly reduced in Erk$^{\Delta IEC}$ intestines, suggesting downregulation of BMP signaling (Fig. 6G). These data suggest that, in IECs, Erk proteins

regulate the expression of hedgehog ligands, which further modulates mesenchymal cells through Bmp signaling.

Inhibition of the Akt/mTor pathway partially rescues the defects in Erk$^{\Delta IEC}$ mice

As rapamycin treatment efficiently suppresses hamartomas in a mouse model of Peutz-Jeghers polyposis (Wei et al., 2008), we investigated whether suppression of mTOR activity could rescue the defects observed in mice lacking Erk in the intestines. Erk$^{\Delta IEC}$ pups were treated with rapamycin from P7 to 4 weeks of age. Rapamycin treatment significantly prolonged the lifespan and increased the survival rate of Erk$^{\Delta IEC}$ mice. All Erk$^{\Delta IEC}$ pups died within 4 weeks; however, after rapamycin treatment, 40% of them survived for the 8 weeks of observation (Fig. 7A). Through histological analysis of intestinal tissues, we found that rapamycin treatment restored the crypt-villus structure and prevented polyp-like defective tissue formation (Fig. 7B), although the villi in rapamycin-treated Erk$^{\Delta IEC}$ mice were still dilated compared with controls. Additionally, Ki67-positive proliferating cells were present only in the crypts of rapamycin-treated Erk$^{\Delta IEC}$ mice and in controls (Fig. 7C). Rapamycin treatment also balanced secretory lineage differentiation in Erk$^{\Delta IEC}$ intestines, as the number of Paneth cells and goblet cells was restored to normal levels (Fig. 7D,E). Ectopic localized Paneth cells were not observed in rapamycin-treated Erk$^{\Delta IEC}$ mice (Fig. 7D). These data suggest that rapamycin treatment prolonged the lifespan of Erk$^{\Delta IEC}$ mice and restored epithelial cell proliferation and differentiation.
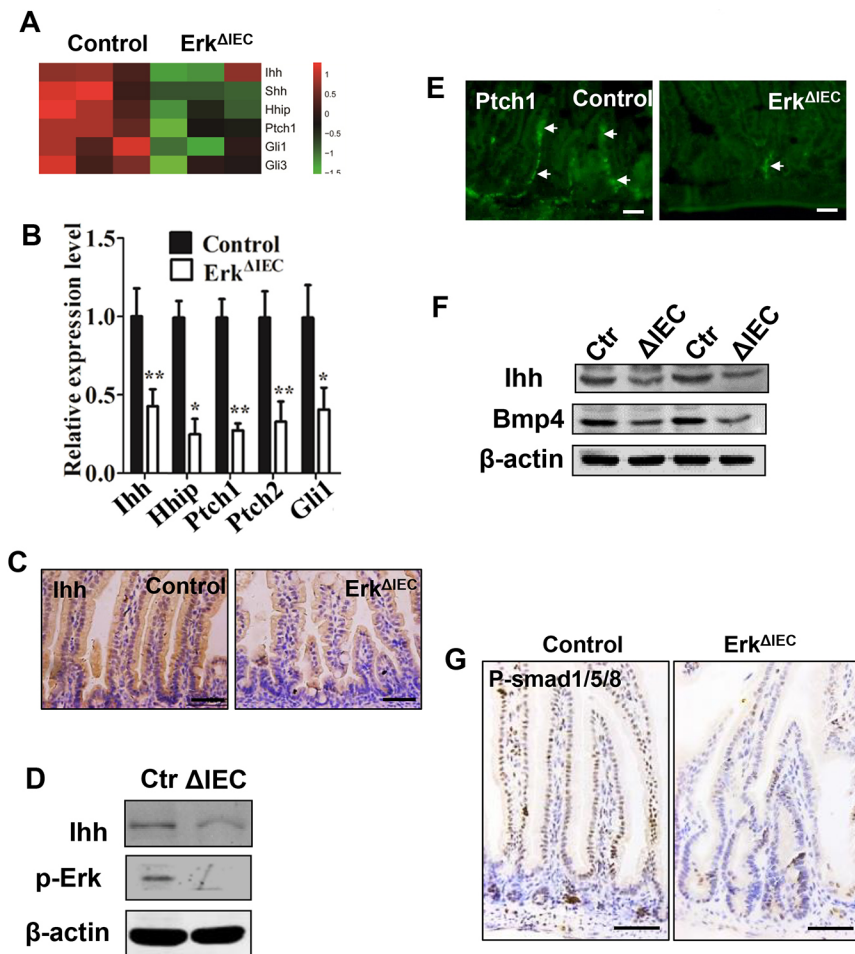
Fig. 6. Loss of Erk1/2 in epithelium impaired Ihh signaling pathway in the intestines. (A) Heat map of hedgehog pathway genes downregulated in Erk$^{\Delta IEC}$ mice from RNA-Seq analysis at P14. (B) Confirmation of hedgehog pathway gene downregulation in Erk$^{\Delta IEC}$ intestines through quantitative RT-PCR analysis. Data are mean±s.e.m. (n=5,*P<0.05, **P<0.01; t-test). (C) Loss of Erk1/2 in intestines reduced the level of Ihh in mice, as determined using immunohistochemistry. (D) Ihh protein levels decreased in Erk$^{\Delta IEC}$ primary cultured organoids. Western blotting was performed using samples harvested from organoids derived from control and Erk$^{\Delta IEC}$ mice. (E) Patched 1 (Ptch1) immunofluorescent staining in small intestine tissues of control and Erk$^{\Delta IEC}$ mice at P6. (F) The protein level of Ihh and Bmp4 was determined by western blotting in intestinal samples harvested from control and Erk$^{\Delta IEC}$ mice at P14. β-Actin was used as a loading control. (G) Ablation of Erk1/2 attenuated Bmp signaling activity. p-Smad1/5/8 immunohistochemical analysis was performed in the small intestines of control and Erk$^{\Delta IEC}$ mice at P14. Scale bars: 50μm.

To further confirm the effect of rapamycin at the molecular level, we examined the p-4E-BP1 levels in rapamycin-treated Erk$^{\Delta IEC}$ intestines and found they were comparable with control mice (Fig. 7F). Hyperactivated Wnt/β-catenin signaling in Erk$^{\Delta IEC}$ intestinal tissues was suppressed by rapamycin treatment, as determined by the level of Wnt downstream targets, such as cyclin D1, Myc and Sox9 (Fig. 7G-I). In addition, rapamycin treatment also increased the protein level of p-Smad1/5/8 in villi of Erk$^{\Delta IEC}$ intestines, suggesting the restoration of the BMP/Smad pathway (Fig. 7J). Consistent with the restoration of BMP signaling, hedgehog downstream targets (but not hedgehog ligands) were also recovered (Fig. 7K), as further supported by the reappearance of α-SMA positive ISEMFs in Erk$^{\Delta IEC}$ mice after rapamycin treatment (Fig. 7L). As Akt is the upstream signal of mTor, an Akt inhibitor should also partially rescue the phenotypes of Erk1/2 deletion in IECs. We tested the effect of an Akt inhibitor (MK-2206) on inhibition of signaling cascades in organoid cultures. MK-2206 inhibited Akt and 4EBP phosphorylation (Fig. S6A). Akt inhibitor treatment significantly decreased the number of Ki67-positive cells compared with control Erk$^{\Delta IEC}$ organoids (Fig. S6B). Moreover, Akt inhibition also partially restored cell differentiation defects in Erk$^{\Delta IEC}$ organoids, such as decreased Paneth cell number and increased goblet cell number (Fig. S6C-G). These data demonstrate that suppression of a hyperactivated Akt-mTor pathway partially rescues Erk deficiency-induced intestinal defects at the histological and molecular level.

DISCUSSION
In this study, we have investigated the role of the MAPK/Erk pathway in IECs during postnatal development. Erk1 and Erk2 are highly

activated in stem/progenitor populations and depletion of Erk1/2 in IECs during prenatal stages surprisingly increases epithelial cell proliferation, crypt dilation, and impaired cell differentiation. More importantly, we have shown for the first time that ablation of Erk1/2 in IECs disrupts intestine morphology, leading to polyp-like structures in a hedgehog-BMP-dependent non-cell-autonomous manner. Erk1/2 deficiency increased the Wnt and Akt-mTor pathways through multiple mechanisms, and suppression of mTor by rapamycin partially rescued cellular and molecular defects, significantly increasing the survival rate of Erk$^{\Delta IEC}$ mice.

Multiple lines of evidence demonstrate that the MAPK pathway plays a crucial role in determining secretory lineage fate in the intestines. Consistent with its upstream regulators, such as Shp2 (Heuberger et al., 2014; Yamashita et al., 2014) and Ras (Feng et al., 2011), Erk also promoted goblet cell and inhibited Paneth cell differentiation, suggesting that this shift is a conserved function of the MAPK pathway. As the most recently defined secretory cell type, Tuft cells do not share common progenitors with goblet and Paneth cells (Gerbe et al., 2011), and the molecular mechanisms for Tuft cell differentiation are largely unknown; however, a recent study has shown that the differentiation of Tuft cells is promoted by Wnt signaling (Ladang et al., 2015). Here, we demonstrated that ERK deficiency induced Wnt hyperactivation but reduced the Tuft cell population, suggesting that Erk signaling is crucial for Tuft cell differentiation downstream of the Wnt pathway.

Hedgehog ligands are secreted by epithelial cells in the intestines to regulate mesenchymal cell development and function, which are crucial for crypt-villus patterning and ISC expansion. We found that Erk$^{\Delta IEC}$ mice phenocopy the mice with a conditional knockout of
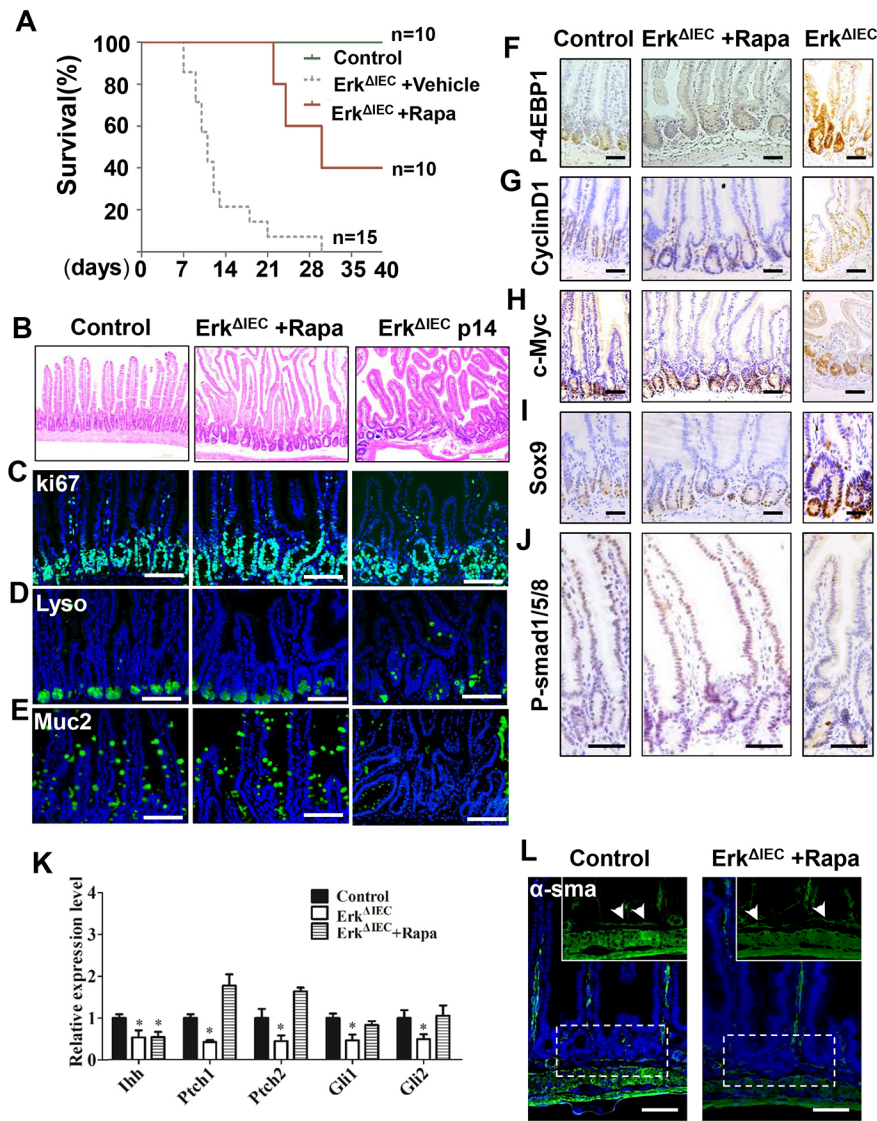
Fig. 7. Inhibition of mTORC1 activity through rapamycin treatment rescued Erk1/2 deficiency-induced defects. (A) Survival rate of control and Erk$^{\Delta IEC}$ mouse strains treated with or without rapamycin (n=10). (B-E) Rapamycin treatment rescued Erk1/2 deficiency-induced cell proliferation and differentiation defects. Untreated Erk$^{\Delta IEC}$ intestines from P14 mice were used as a mutant control. Wild-type control and Erk$^{\Delta IEC}$ mice were treated with rapamycin from P7 for 4 weeks. Histological (B) and immunofluorescent analysis for Ki67 (C), lysozyme (D) and mucin 2 (E) in the intestines of control and Erk$^{\Delta IEC}$ littermates at indicated time points. (F-J) Rapamycin treatment restored downstream signaling in Erk$^{\Delta IEC}$ mice. Immunohistochemical analysis of p-4EBP1 (F), cyclin D1 (G), Myc (H), Sox9 (I) and p-Smad1/5/8 (J) in intestines of control and Erk$^{\Delta IEC}$ littermates treated with rapamycin for 3 weeks. (K) Rapamycin treatment restored the expression of Ihh pathway downstream targets in Erk$^{\Delta IEC}$ mice. qPCR analysis of mRNA levels of hedgehog signaling pathway genes in intestines of control and Erk$^{\Delta IEC}$ littermates treated with or without rapamycin for 3 weeks. Data are mean±s.e.m. (n=3, *$P<0.05$; t-test). (L) Reappearance of ISEMFs in Erk$^{\Delta IEC}$ intestinal tissues after rapamycin treatment for 3 weeks. α-SMA immunostaining analysis of muscularis mucosae cells in control and Erk$^{\Delta IEC}$ small intestines. Scale bars: 100 µm in B,F-J; 50 µm in C-E,L.

Ihh, the key hedgehog ligand in intestine development (Kosinski et al., 2010; van Dop et al., 2010). Shh has been shown to play mild roles in IEC proliferation and secretory lineage differentiation, but specific deletion of Shh in mouse IECs does not affect intestinal morphology (Gagne-Sansfacon et al., 2014). Thus, we believe Erk mainly affected Ihh signaling. More importantly, downregulation of the Bmp4-Smad pathway and activation of Wnt signaling were observed in Erk$^{\Delta IEC}$ mice, which is consistent with intestinal-specific deletion of Ihh in mice (van Dop et al., 2010). We found that the expression of Ihh was downregulated in Erk1/2-deficient tissue and organoids, suggesting the regulation is through a cell-autonomous manner. Our study demonstrates a previously uncovered connection between MAPK/ERK signaling and the hedgehog pathway in intestinal development.

The crosstalk between Wnt and MAPK signaling is complicated under both physiological and pathological conditions. It is well accepted that Wnt and MAPK/ERK are mutually activating pathways in colorectal cancer. For example, Wnt signaling induces MAPK/ERK pathway through stabilization of Ras protein (Jeong et al., 2012) and MAPK/ERK activates Wnt signaling through phosphorylation of LRP6 and other mechanisms (Lemieux et al., 2015; Ji et al., 2009; Cervenka et al., 2011). However, growing evidence has demonstrated

negative regulation mechanisms between these two pathways, especially during homeostasis. Using IECs as a model, a study suggests that Shp2/MAPK signaling inhibits the Wnt pathway potentially due to increased stability of a shorter TCF4 (TCF4M/S) splice variant, which produces a dominant-negative truncation (Heuberger et al., 2014). Using PORCN inhibitor to acutely suppress Wnt signaling in vivo, it has been reported that the Wnt pathway suppresses the MAPK cascade to maintain a stable pool of ISC (Kabiri et al., 2018). Here, we also found that the Erk pathway restrains Wnt signaling activity to maintain cell migration and differentiation in the intestines, through more-complicated mechanisms in both cell-autonomous and non-autonomous manners. First, epithelial Erk1/2 stimulated the Ihh level, activating the Hh pathway to enhance BMP production and ultimately restrain Wnt/β-catenin. In addition, we found that deletion of Erk1/2 resulted in activation of the PI3 K/Akt pathway, which has been shown to activate Wnt/β-catenin through inhibition of Gsk-3β and direct phosphorylation of β-catenin at Ser552 to activate β-catenin (Lee et al., 2010; He et al., 2007; Nusse and Clevers, 2017). However, depletion of Erk1/2 in adult IECs did not show upregulation of Wnt/β-catenin signaling (de Jong et al., 2016), further suggesting that the MAPK/Erk pathway regulates Wnt signaling in a developmental

stage-dependent manner. Our study is consistent with a recent report demonstrating that pharmacological inhibition of MEK/Erk activates the Wnt pathway and expands the stem cell population in colorectal cancer through inhibition of Egr1-mediated Axin1 expression (Zhan et al., 2019). These studies, including ours, suggest that inhibition of MAPK/ERK signaling eventually activates Wnt signaling in intestinal development and cancer through multiple mechanisms.

Deletion of Erk1/2 activated the Ras/Raf/Mek cascade owing to loss of Erk1/2-dependent negative feedback regulation, leading to transactivation of Akt/mTor signaling in the intestines. Activation of mTor inhibited secretory cell lineage differentiation due to increased Notch activity (Zhou et al., 2015). Using rapamycin to treat Erk IEC mice rescued secretory lineage differentiation. In addition, rapamycin treatment also restored intestinal architecture and significantly increased the survival rate of Erk$^{\Delta IEC}$ mice. Although we found the expression level of Ihh target genes was restored, Ihh expression was not recovered in Erk$^{\Delta IEC}$ mice after rapamycin treatment, suggesting that rapamycin activates the Hh pathway in mesenchymal cells through an unrevealed mechanism.

In summary, we demonstrate that Erk1/2 signaling is crucial for intestinal development and ISC homeostasis. Through our current study, we provide evidence that the ERK/MAPK pathway crosstalks with the Hh and Wnt pathways, suggesting that ERK1/2 are crucial factors that integrate cell fate decision signaling during intestinal development. Given that inhibition of MAPK in cancers usually activates multiple oncogenic pathways (Lake et al., 2016), our findings also demonstrate the complicated feedback loop operating during normal tissue development. Further elucidation of the exact molecular mechanisms of this feedback regulation will improve the understanding of intestinal homeostasis and tumorigenesis.

MATERIALS AND METHODS
Mice and treatments
All mice were bred and maintained in specific pathogen-free conditions in the animal facilities of East China Normal University, Shanghai. *Erk1$^{-/-}$* and *Erk2$^{flox/flox}$* mice were a gift from Dr Hengyu Fan (Life Sciences Institute, Zhejiang University, China). Villin-Cre mice were obtained from the National Resource Center of Mutant Mice (NRCMM), and *Lgr5-eGFP-IRES-CreERT2* mice were obtained from the Jackson Laboratory. For rapamycin treatment, 7-day-old mice were treated by intraperitoneal injection of 2 mg/kg/day for 28 days. All experiments conformed to the regulations drafted by the Association for Assessment and Accreditation of Laboratory Animal Care in Shanghai and were approved by the East China Normal University Centre for Animal Research (protocol number AR2013/12008).

Histology, immunohistochemistry and immunofluorescence
The intestines were fixed in 4% paraformaldehyde, dehydrated and embedded in paraffin. For immunohistochemistry staining, after antigen retrieval, the sections were blocked with 1% BSA and incubated with primary antibody overnight at 4°C. After incubation with secondary antibody, sections were developed with DAB reagent, counterstained with Hematoxylin, dehydrated and mounted in neutral resin. Primary antibodies and their dilutions were as follows: p-Erk1/2 (1:100, Cell Signaling Technology, 4370); GFP (1:100, Santa Cruz Biotechnology, sc-101525); Ki67 (1:2000, NeoMarker, rm-9106); lysozyme (1:2000; Dako, A009902); Muc2 (1:50, Santa Cruz Biotechnology, sc-15334); chromogranin A (1:2000, Immunostar, 20085); Dclk1(1:100, Abcam, ab31704); BrdU (1:500, Abcam, ab8152); β-catenin (1:100, BD Transduction Laboratories, 610154); c-Myc (1:100, Santa Cruz Biotechnology, sc-40); Sox9 (1:500, Abcam, ab185966); p-4EBP1 (1:400, Cell Signaling Technology, 2855); p-S6 (1:400, Cell Signaling Technology, 4858); p-Akt (1:100, Cell Signaling Technology, 3787); Ihh (1:50, Santa Cruz Biotechnology, sc-13088); Ptch1 (1:100; Santa Cruz Biotechnology, sc-518102); p-Smad1/5/8 (1:100, Cell Signaling Technology, 13820); and α-SMA (1:50, Abcam, ab5694). For quantitative analysis, cell counting was performed in at least ten sections from three or more mice for each genotype.

Immunoblotting
A small piece of proximal duodenum was rinsed with ice-cold PBS and lysed in ice-cold lysis buffer. Protein extracts were quantified by Micro BCA Protein Assay Kit (Thermo Scientific) and resolved by SDS-PAGE. Primary antibodies were as follows: β-actin (1:5000, Sigma-Aldrich, A5441); Ihh (1:500, Santa Cruz Biotechnology, sc-13088); Bmp4 (1:500, Abcam, ab39973); Erk1/2, p-Erk1/2, Akt, p-Akt, S6K1, p-S6K1, 4EBP1, p-4EBP1, Egfr, p-Egfr, Ras, Ras-GTP, Raf, p-Raf, Mek1/2, p-Mek1(s217/221) and cyclin D1 (1:1000, Cell Signaling Technology, 4695, 4370, 4685, 3787, 2708, 9206, 9644, 2855, 4267, 3777, 3339, 8821, 9422, 9421, 9122, 9121, 2978, respectively).

Small intestinal crypt isolation and organoid culture
Crypts were released from murine small intestine and mixed with 50 μl of Matrigel (BD Bioscience) in 96-well plates. 100 μl of basic culture medium containing growth factors (50 ng/ml EGF, 500 ng/ml R-spondin1 and 100 ng/ml Noggin, all from Peprotech) was added. Organoid growth was quantified by scoring the number of buds and Edu$^+$ cells on microscopic images from at least 90 organoids from three or more mice for each genotype. For small-molecule treatment, the following inhibitors were used: MK2206 (500 nM; SelleckChem, HY-108232). Paraffin sections were generated and analyzed by immunofluorescence staining.

Quantitative RT-PCR
Total RNA was extracted from a small piece of proximal duodenum tissue using Trizol reagent (Invitrogen). DNA was synthesized with the Superscript RNase H2Reverse Transcriptase Kit (Takara) using 2.5 mM random hexamers (Takara). Real-time PCR was performed using the SYBR Green PCR Kit (Takara) on a Mx3005P thermal cycler (Stratagene) and actin was used as an internal control.

In situ hybridization
Tissue slides were deparaffinized, rehydrated and washed in PBS. After pretreatment with 0.2 N HCl and proteinase K, slides were post-fixed in 4% paraformaldehyde. Slides were washed and placed in fresh acetic anhydride solution then washed with PBS and rinsed in 5×SSC. Slides were placed in a box humidified with 5×SSC (pH 7.5)/50% formamide, then hybridization solution was added and the slides incubated in a box at 65°C for at least 1 h. The slides were supplied with hybridization solution containing 500 ng/ml of digoxigenin-labeled probe and incubated at 72°C for 48 h. The slides were then washed in SSC buffers and incubated with anti-Dig antibody overnight at 4°C. Sections were subsequently washed and colored with NCBI/NBT (Roche) for 12 h at room temperature in the darkness, then dehydrated and mounted with neutral resins.

Electron microscopy
Small intestinal tissue samples were fixed with 2.5% glutaraldehyde and post-fixed in 1% osmium tetroxide. For scanning EM, tissue was dehydrated and dried using the CO$_2$ critical point method. The dried samples were bonded to a metal sample stage and then sputtered onto a layer of metallic film in a vacuum evaporator. The villus structure was assessed by scanning EM.

Transmission electron microscopy
Small intestinal samples were fixed with 2% paraformaldehyde with 2.5% glutaraldehyde and post-fixed in 1% osmium tetroxide in 100 mM phosphate buffer. Tissue was dehydrated, embedded in epoxy resin and sectioned for placement on TEM grids. Images were captured with a JEOL transmission electron microscope at 120 kV (model JEM-1210).

RNA-seq analysis
Small intestines of 14-day-old control and Erk$^{\Delta IEC}$ mice were removed, flash frozen on dry ice and RNA was harvested using Trizol reagent. Illumina TruSeq RNA Sample Prep Kit was used with 1 μg of total RNA for the construction of sequencing libraries. The RNA libraries were then sequenced on Illumina Hiseq 2000 platform and 125 bp paired-end reads were generated. RNA-seq data were separately aligned to the mouse reference genome mm10 using Tophat2 (version 2.1.0) and the expression levels of all genes were

estimated by the program 'htseq-count' in HTSeq software (version 0.6.0). GSEA analyses presented in this article were performed by Java GSEA implementation (version 3.0). RNA-seq raw data and processed data of this project have been submitted to GEO under accession number GSE134249.

Statistical analysis

Statistical analyses were performed with Prism GraphPad software. Data are expressed as mean±s.e.m. Unpaired two-tailed Student's *t*-test or one-way ANOVA was used for statistical comparison of means, with *P*<0.05 defined as statistically significant. Unless indicated in the figure legends, all the experiments were performed at least three times with similar results.

Competing interests
The authors declare no competing or financial interests.

Author contributions
Conceptualization: G.W., N.G., L.L., X.P., H.C., M.L., X.Z., D.L.; Methodology: G.W., N.G., J.C., L.F., X.P., H.C., M.L., X.Z., D.L.; Software: G.W., N.G., J.C., L.F., Z.Z., L.L.; Validation: G.W., N.G., L.F., Z.Z., D.L.; Formal analysis: G.W., N.G., J.C., L.F., Z.Z., G.G., L.L., G.F., K.H., X.P., M.L., X.Z., D.L.; Investigation: G.W., N.G., J.C., Z.Z., G.G., M.L., X.Z., D.L.; Resources: H.-Y.F., D.L.; Data curation: G.W., J.C., L.F., Z.Z., G.G., G.F., K.H., H.-Y.F., M.L., X.Z., D.L.; Writing - original draft: G.W., D.L.; Writing - review & editing: G.W., D.L.; Visualization: D.L.; Supervision: G.W., M.L., D.L.; Project administration: M.L., D.L.; Funding acquisition: M.L., D.L.

Data availability
RNA-seq raw data and processed data of this project have been submitted to GEO under accession number GSE134249.

Supplementary information
Supplementary information available online at
https://dev.biologists.org/lookup/doi/10.1242/dev.185678.supplemental

References
Akiyoshi, T., Nakamura, M., Koga, K., Nakashima, H., Yao, T., Tsuneyoshi, M., Tanaka, M. and Katano, M. (2006). Gli1, downregulated in colorectal cancers, inhibits proliferation of colon cancer cells involving Wnt signalling activation. *Gut* **55**, 991-999. doi:10.1136/gut.2005.080333

Ayyaz, A., Kumar, S., Sangiorgi, B., Ghoshal, B., Gosio, J., Ouladan, S., Fink, M., Barutcu, S., Trcka, D., Shen, J. et al. (2019). Single-cell transcriptomes of the regenerating intestine reveal a revival stem cell. *Nature* **569**, 121-125. doi:10.1038/s41586-019-1154-y

Barker, N., Van Es, J. H., Kuipers, J., Kujala, P., Van Den Born, M., Cozijnsen, M., Haegebarth, A., Korving, J., Begthel, H., Peters, P. J. and et al. (2007). Identification of stem cells in small intestine and colon by marker gene Lgr5. *Nature* **449**, 1003-1007. doi:10.1038/nature06196

Blalock, W. L., Navolanic, P. M., Steelman, L. S., Shelton, J. G., Moye, P. W., Lee, J. T., Franklin, R. A., Mirza, A., Mcmahon, M., White, M. K. and et al. (2003). Requirement for the PI3K/Akt pathway in MEK1-mediated growth and prevention of apoptosis: identification of an Achilles heel in leukemia. *Leukemia* **17**, 1058-1067. doi:10.1038/sj.leu.2402925

Cervenka, I., Wolf, J., Masek, J., Krejci, P., Wilcox, W. R., Kozubik, A., Schulte, G., Gutkind, J. S. and Bryja, V. (2011). Mitogen-activated protein kinases promote WNT/beta-catenin signaling via phosphorylation of LRP6. *Mol. Cell. Biol.* **31**, 179-189. doi:10.1128/MCB.00550-10

Clevers, H. (2013). The intestinal crypt, a prototype stem cell compartment. *Cell* **154**, 274-284. doi:10.1016/j.cell.2013.07.004

de Jong, P. R., Taniguchi, K., Harris, A. R., Bertin, S., Takahashi, N., Duong, J., Campos, A. D., Powis, G., Corr, M., Karin, M. et al. (2016). ERK5 signalling rescues intestinal epithelial turnover and tumour cell proliferation upon ERK1/2 abrogation. *Nat. Commun.* **7**, 11551. doi:10.1038/ncomms11551

Fan, H. Y., Liu, Z., Shimada, M., Sterneck, E., Johnson, P. F., Hedrick, S. M. and Richards, J. S. (2009). MAPK3/1 (ERK1/2) in ovarian granulosa cells are essential for female fertility. *Science* **324**, 938-941. doi:10.1126/science.1171396

Feng, Y., Bommer, G. T., Zhao, J., Green, M., Sands, E., Zhai, Y., Brown, K., Burberry, A., Cho, K. R. and Fearon, E. R. (2011). Mutant KRAS promotes hyperplasia and alters differentiation in the colon epithelium but does not expand the presumptive stem cell pool. *Gastroenterology* **141**, 1003-1013.e10. doi:10.1053/j.gastro.2011.05.007

Fischer, A. M., Katayama, C. D., Pagès, G., Pouysségur, J. and Hedrick, S. M. (2005). The role of erk1 and erk2 in multiple stages of T cell development. *Immunity* **23**, 431-443. doi:10.1016/j.immuni.2005.08.013

Fre, S., Pallavi, S. K., Huyghe, M., Lae, M., Janssen, K. P., Robine, S., Artavanis-Tsakonas, S. and Louvard, D. (2009). Notch and Wnt signals cooperatively control cell proliferation and tumorigenesis in the intestine. *Proc. Natl. Acad. Sci. USA* **106**, 6309-6314. doi:10.1073/pnas.0900427106

Gagne-Sansfacon, J., Allaire, J. M., Jones, C., Boudreau, F. and Perreault, N. (2014). Loss of Sonic hedgehog leads to alterations in intestinal secretory cell maturation and autophagy. *PLoS ONE* **9**, e98751. doi:10.1371/journal.pone.0098751

Galceran, J., Sustmann, C., Hsu, S. C., Folberth, S. and Grosschedl, R. (2004). LEF1-mediated regulation of Delta-like1 links Wnt and Notch signaling in somitogenesis. *Genes Dev.* **18**, 2718-2723. doi:10.1101/gad.1249504

Gerbe, F., Van Es, J. H., Makrini, L., Brulin, B., Mellitzer, G., Robine, S., Romagnolo, B., Shroyer, N. F., Bourgaux, J. F., Pignodel, C. et al. (2011). Distinct ATOH1 and Neurog3 requirements define tuft cells as a new secretory cell type in the intestinal epithelium. *J. Cell Biol.* **192**, 767-780. doi:10.1083/jcb.201010127

Gerbe, F., Sidot, E., Smyth, D. J., Ohmoto, M., Matsumoto, I., Dardalhon, V., Cesses, P., Garnier, L., Pouzolles, M., Brulin, B. et al. (2016). Intestinal epithelial tuft cells initiate type 2 mucosal immunity to helminth parasites. *Nature* **529**, 226-230. doi:10.1038/nature16527

Haber, A. L., Biton, M., Rogel, N., Herbst, R. H., Shekhar, K., Smillie, C., Burgin, G., Delorey, T. M., Howitt, M. R., Katz, Y. et al. (2017). A single-cell survey of the small intestinal epithelium. *Nature* **551**, 333-339. doi:10.1038/nature24489

Haigis, K. M., Kendall, K. R., Wang, Y., Cheung, A., Haigis, M. C., Glickman, J. N., Niwa-Kawakita, M., Sweet-Cordero, A., Sebolt-Leopold, J., Shannon, K. M. et al. (2008). Differential effects of oncogenic K-Ras and N-Ras on proliferation, differentiation and tumor progression in the colon. *Nat. Genet.* **40**, 600-608. doi:10.1038/ng.115

Haramis, A. P., Begthel, H., Van Den Born, M., Van Es, J., Jonkheer, S., Offerhaus, G. J. and Clevers, H. (2004). De novo crypt formation and juvenile polyposis on BMP inhibition in mouse intestine. *Science* **303**, 1684-1686. doi:10.1126/science.1093587

He, X. C., Zhang, J., Tong, W. G., Tawfik, O., Ross, J., Scoville, D. H., Tian, Q., Zeng, X., He, X., Wiedemann, L. M. et al. (2004). BMP signaling inhibits intestinal stem cell self-renewal through suppression of Wnt-beta-catenin signaling. *Nat. Genet.* **36**, 1117-1121. doi:10.1038/ng1430

He, X. C., Yin, T., Grindley, J. C., Tian, Q., Sato, T., Tao, W. A., Dirisina, R., Porter-Westpfahl, K. S., Hembree, M., Johnson, T. et al. (2007). PTEN-deficient intestinal stem cells initiate intestinal polyposis. *Nat. Genet.* **39**, 189-198. doi:10.1038/ng1928

Heuberger, J., Kosel, F., Qi, J., Grossmann, K. S., Rajewsky, K. and Birchmeier, W. (2014). Shp2/MAPK signaling controls goblet/paneth cell fate decisions in the intestine. *Proc. Natl. Acad. Sci. USA* **111**, 3472-3477. doi:10.1073/pnas.1309342111

Jeong, W.-J., Yoon, J., Park, J.-C., Lee, S.-H., Lee, S.-H., Kaduwal, S., Kim, H., Yoon, J.-B. and Choi, K.-Y. (2012). Ras stabilization through aberrant activation of Wnt/beta-catenin signaling promotes intestinal tumorigenesis. *Sci. Signal.* **5**, ra30. doi:10.1126/scisignal.2002242

Ji, H., Wang, J., Nika, H., Hawke, D., Keezer, S., Ge, Q., Fang, B., Fang, X., Fang, D., Litchfield, D. W. et al. (2009). EGF-induced ERK activation promotes CK2-mediated disassociation of alpha-Catenin from beta-Catenin and transactivation of beta-Catenin. *Mol. Cell* **36**, 547-559. doi:10.1016/j.molcel.2009.09.034

Kabiri, Z., Greicius, G., Zaribafzadeh, H., Hemmerich, A., Counter, C. M. and Virshup, D. M. (2018). Wnt signaling suppresses MAPK-driven proliferation of intestinal stem cells. *J. Clin. Invest.* **128**, 3806-3812. doi:10.1172/JCI99325

Kosinski, C., Stange, D. E., Xu, C., Chan, A. S., Ho, C., Yuen, S. T., Mifflin, R. C., Powell, D. W., Clevers, H., Leung, S. Y. et al. (2010). Indian hedgehog regulates intestinal stem cell fate through epithelial-mesenchymal interactions during development. *Gastroenterology* **139**, 893-903. doi:10.1053/j.gastro.2010.06.014

Ladang, A., Rapino, F., Heukamp, L. C., Tharun, L., Shostak, K., Hermand, D., Delaunay, S., Klevernic, I., Jiang, Z., Jacques, N. et al. (2015). Elp3 drives Wnt-dependent tumor initiation and regeneration in the intestine. *J. Exp. Med.* **212**, 2057-2075. doi:10.1084/jem.20142288

Lake, D., Correa, S. A. and Muller, J. (2016). Negative feedback regulation of the ERK1/2 MAPK pathway. *Cell. Mol. Life Sci.* **73**, 4397-4413. doi:10.1007/s00018-016-2297-8

DEVELOPMENT

Lee, G., Goretsky, T., Managlia, E., Dirisina, R., Singh, A. P., Brown, J. B., May, R., Yang, G.-Y., Ragheb, J. W., Evers, B. M. et al. (2010). Phosphoinositide 3-kinase signaling mediates beta-catenin activation in intestinal epithelial stem and progenitor cells in colitis. Gastroenterology 139, 869-81.e9. doi:10.1053/j.gastro.2010.05.037

Lemieux, E., Cagnol, S., Beaudry, K., Carrier, J. and Rivard, N. (2015). Oncogenic KRAS signalling promotes the Wnt/beta-catenin pathway through LRP6 in colorectal cancer. Oncogene 34, 4914-4927. doi:10.1038/onc.2014.416

Liu, S., Qian, Y., Li, L., Wei, G., Guan, Y., Pan, H., Guan, X., Zhang, L., Lu, X., Zhao, Y. et al. (2013). Lgr4 gene deficiency increases susceptibility and severity of dextran sodium sulfate-induced inflammatory bowel disease in mice. J. Biol. Chem. 288, 8794-8803. doi:10.1074/jbc.M112.436204

Madison, B. B., Dunbar, L., Qiao, X. T., Braunstein, K., Braunstein, E. and Gumucio, D. L. (2002). Cis elements of the villin gene control expression in restricted domains of the vertical (crypt) and horizontal (duodenum, cecum) axes of the intestine. J. Biol. Chem. 277, 33275-33283. doi:10.1074/jbc.M204935200

Madison, B. B., Braunstein, K., Kuizon, E., Portman, K., Qiao, X. T. and Gumucio, D. L. (2005). Epithelial hedgehog signals pattern the intestinal crypt-villus axis. Development 132, 279-289. doi:10.1242/dev.01576

Miettinen, P. J., Berger, J. E., Meneses, J., Phung, Y., Pedersen, R. A., Werb, Z. and Derynck, R. (1995). Epithelial immaturity and multiorgan failure in mice lacking epidermal growth factor receptor. Nature 376, 337-341. doi:10.1038/376337a0

Munoz, J., Stange, D. E., Schepers, A. G., Van De Wetering, M., Koo, B. K., Itzkovitz, S., Volckmann, R., Kung, K. S., Koster, J., Radulescu, S. et al. (2012). The Lgr5 intestinal stem cell signature: robust expression of proposed quiescent '+4' cell markers. EMBO J. 31, 3079-3091. doi:10.1038/emboj.2012.166

Nusse, R. and Clevers, H. (2017). Wnt/β-catenin signaling, disease, and emerging therapeutic modalities. Cell 169, 985-999. doi:10.1016/j.cell.2017.05.016

Pages, G., Guerin, S., Grall, D., Bonino, F., Smith, A., Anjuere, F., Auberger, P. and Pouyssegur, J. (1999). Defective thymocyte maturation in p44 MAP kinase (Erk 1) knockout mice. Science 286, 1374-1377. doi:10.1126/science.286.5443.1374

Prahallad, A., Sun, C., Huang, S., Di Nicolantonio, F., Salazar, R., Zecchin, D., Beijersbergen, R. L., Bardelli, A. and Bernards, R. (2012). Unresponsiveness of colon cancer to BRAF(V600E) inhibition through feedback activation of EGFR. Nature 483, 100-103. doi:10.1038/nature10868

Ramalho-Santos, M., Melton, D. A. and Mcmahon, A. P. (2000). Hedgehog signals regulate multiple aspects of gastrointestinal development. Development 127, 2763-2772.

Roberts, D. J., Johnson, R. L., Burke, A. C., Nelson, C. E., Morgan, B. A. and Tabin, C. (1995). Sonic hedgehog is an endodermal signal inducing Bmp-4 and Hox genes during induction and regionalization of the chick hindgut. Development 121, 3163-3174.

Rodilla, V., Villanueva, A., Obrador-Hevia, A., Robert-Moreno, A., Fernandez-Majada, V., Grilli, A., Lopez-Bigas, N., Bellora, N., Alba, M. M., Torres, F. et al. (2009). Jagged1 is the pathological link between Wnt and Notch pathways in colorectal cancer. Proc. Natl. Acad. Sci. USA 106, 6315-6320. doi:10.1073/pnas.0813221106

Sangiorgi, E. and Capecchi, M. R. (2008). Bmi1 is expressed in vivo in intestinal stem cells. Nat. Genet. 40, 915-920. doi:10.1038/ng.165

Sansom, O. J., Reed, K. R., Hayes, A. J., Ireland, H., Brinkmann, H., Newton, I. P., Batlle, E., Simon-Assmann, P., Clevers, H., Nathke, I. S. et al. (2004). Loss of Apc in vivo immediately perturbs Wnt signaling, differentiation, and migration. Genes Dev. 18, 1385-1390. doi:10.1101/gad.287404

Sato, T., Vries, R. G., Snippert, H. J., Van De Wetering, M., Barker, N., Stange, D. E., Van Es, J. H., Abo, A., Kujala, P., Peters, P. J. et al. (2009). Single Lgr5 stem cells build crypt-villus structures in vitro without a mesenchymal niche. Nature 459, 262-265. doi:10.1038/nature07935

Sato, T., Van Es, J. H., Snippert, H. J., Stange, D. E., Vries, R. G., Van Den Born, M., Barker, N., Shroyer, N. F., Van De Wetering, M. and Clevers, H. (2011). Paneth cells constitute the niche for Lgr5 stem cells in intestinal crypts. Nature 469, 415-418. doi:10.1038/nature09637

Trobridge, P., Knoblaugh, S., Washington, M. K., Munoz, N. M., Tsuchiya, K. D., Rojas, A., Song, X., Ulrich, C. M., Sasazuki, T., Shirasawa, S. et al. (2009).

TGF-β receptor inactivation and mutant Kras induce intestinal neoplasms in mice via a beta-catenin-independent pathway. Gastroenterology 136, 1680-1688.e7. doi:10.1053/j.gastro.2009.01.066

Van Der Flier, L. G., Sabates-Bellver, J., Oving, I., Haegebarth, A., De Palo, M., Anti, M., Van Gijn, M. E., Suijkerbuijk, S., Van De Wetering, M., Marra, G. and et al. (2007). The Intestinal Wnt/TCF Signature. Gastroenterology 132, 628-632. doi:10.1053/j.gastro.2006.08.039

Van der Flier, L. G., Van Gijn, M. E., Hatzis, P., Kujala, P., Haegebarth, A., Stange, D. E., Begthel, H., Van Den Born, M., Guryev, V., Oving, I. et al. (2009). Transcription factor achaete scute-like 2 controls intestinal stem cell fate. Cell 136, 903-912. doi:10.1016/j.cell.2009.01.031

Van Dop, W. A., Uhmann, A., Wijgerde, M., Sleddens-Linkels, E., Heijmans, J., Offerhaus, G. J., Van Den Bergh Weerman, M. A., Boeckxstaens, G. E., Hommes, D. W., Hardwick, J. C. et al. (2009). Depletion of the colonic epithelial precursor cell compartment upon conditional activation of the hedgehog pathway. Gastroenterology 136, 2195-2203.e7. doi:10.1053/j.gastro.2009.02.068

Van Dop, W. A., Heijmans, J., Büller, N. V. J. A., Snoek, S. A., Rosekrans, S. L., Wassenberg, E. A., Van Den Bergh Weerman, M. A., Lanske, B., Clarke, A. R., Winton, D. J. et al. (2010). Loss of Indian Hedgehog activates multiple aspects of a wound healing response in the mouse intestine. Gastroenterology 139, 1665-1676.e1-10. doi:10.1053/j.gastro.2010.07.045

Van Es, J. H., Jay, P., Gregorieff, A., Van Gijn, M. E., Jonkheer, S., Hatzis, P., Thiele, A., Van Den Born, M., Begthel, H., Brabletz, T. et al. (2005a). Wnt signalling induces maturation of Paneth cells in intestinal crypts. Nat. Cell Biol. 7, 381-386. doi:10.1038/ncb1240

van Es, J. H., Van Gijn, M. E., Riccio, O., van den Born, M., Vooijs, M., Begthel, H., Cozijnsen, M., Robine, S., Winton, D. J., Radtke, F. and et al. (2005b). Notch/γ-secretase inhibition turns proliferative cells in intestinal crypts and adenomas into goblet cells. Nature 435, 959-963. doi:10.1038/nature03659

Van Es, J. H., Sato, T., Van De Wetering, M., Lyubimova, A., Nee, A. N., Gregorieff, A., Sasaki, N., Zeinstra, L., Van Den Born, M., Korving, J. et al. (2012). Dll1+ secretory progenitor cells revert to stem cells upon crypt damage. Nat. Cell Biol. 14, 1099-1010. doi:10.1038/ncb2581

Visvader, J. E. and Clevers, H. (2016). Tissue-specific designs of stem cell hierarchies. Nat. Cell Biol. 18, 349-355. doi:10.1038/ncb3332

Wei, C., Amos, C. I., Zhang, N., Wang, X., Rashid, A., Walker, C. L., Behringer, R. R. and Frazier, M. L. (2008). Suppression of Peutz-Jeghers polyposis by targeting mammalian target of rapamycin signaling. Clin. Cancer Res. 14, 1167-1171. doi:10.1158/1078-0432.CCR-07-4007

Wong, V. W., Stange, D. E., Page, M. E., Buczacki, S., Wabik, A., Itami, S., Van De Wetering, M., Poulsom, R., Wright, N. A., Trotter, M. W. et al. (2012). Lrig1 controls intestinal stem-cell homeostasis by negative regulation of ErbB signalling. Nat. Cell Biol. 14, 401-408. doi:10.1038/ncb2464

Yamashita, H., Kotani, T., Park, J. H., Murata, Y., Okazawa, H., Ohnishi, H., Ku, Y. and Matozaki, T. (2014). Role of the protein tyrosine phosphatase Shp2 in homeostasis of the intestinal epithelium. PLoS ONE 9, e92904. doi:10.1371/journal.pone.0092904

Yao, Y., Li, W., Wu, J., Germann, U. A., Su, M. S., Kuida, K. and Boucher, D. M. (2003). Extracellular signal-regulated kinase 2 is necessary for mesoderm differentiation. Proc. Natl. Acad. Sci. USA 100, 12759-12764. doi:10.1073/pnas.2134254100

Zbuk, K. M. and Eng, C. (2007). Hamartomatous polyposis syndromes. Nat. Clin. Pract. Gastroenterol. Hepatol. 4, 492-502. doi:10.1038/ncpgasthep0902

Zhan, T., Ambrosi, G., Wandmacher, A. M., Rauscher, B., Betge, J., Rindtorff, N., Haussler, R. S., Hinsenkamp, I., Bamberg, L., Hessling, B. et al. (2019). MEK inhibitors activate Wnt signalling and induce stem cell plasticity in colorectal cancer. Nat. Commun. 10, 2197. doi:10.1038/s41467-019-09898-0

Zhou, Y., Rychahou, P., Wang, Q., Weiss, H. L. and Evers, B. M. (2015). TSC2/mTORC1 signaling controls Paneth and goblet cell differentiation in the intestinal epithelium. Cell Death Dis. 6, e1631. doi:10.1038/cddis.2014.588

Zmajkovicova, K., Jesenberger, V., Catalanotti, F., Baumgartner, C., Reyes, G. and Baccarini, M. (2013). MEK1 is required for PTEN membrane recruitment, AKT regulation, and the maintenance of peripheral tolerance. Mol. Cell 50, 43-55. doi:10.1016/j.molcel.2013.01.037